the FEBS Journal

The autophagic response to nutrient deprivation in the hl-1 cardiac myocyte is modulated by Bcl-2 and sarco/endoplasmic reticulum calcium stores

Nathan R. Brady[1], Anne Hamacher-Brady[1], Hua Yuan[1,2] and Roberta A. Gottlieb[1,2]

1 Department of Molecular and Experimental Medicine, The Scripps Research Institute, La Jolla, CA, USA
2 BioScience Center, San Diego State University, CA, USA

Keywords
autophagy; Bcl-2; Beclin 1; HL-1 cardiac myocyte; GFP-LC3

Correspondence
R. A. Gottlieb, BioScience Center, San Diego State University, 5500 Campanile Drive, San Diego, CA 92182-4650, USA
Fax: +1 619 594 8984
Tel: +1 619 594 8981
E-mail: robbieg@sciences.sdsu.edu

(Received 17 July 2006, revised 23 April 2007, accepted 27 April 2007)

doi:10.1111/j.1742-4658.2007.05849.x

Macroautophagy is a vital process in the cardiac myocyte: it plays a protective role in the response to ischemic injury, and chronic perturbation is causative in heart disease. Recent findings evidence a link between the apoptotic and autophagic pathways through the interaction of the anti-apoptotic proteins Bcl-2 and Bcl-X_L with Beclin 1. However, the nature of the interaction, either in promoting or blocking autophagy, remains unclear. Here, using a highly sensitive, macroautophagy-specific flux assay allowing for the distinction between enhanced autophagosome production and suppressed autophagosome degradation, we investigated the control of Beclin 1 and Bcl-2 on nutrient deprivation-activated macroautophagy. We found that in HL-1 cardiac myocytes the relationship between Beclin 1 and Bcl-2 is subtle: Beclin 1 mutant lacking the Bcl-2-binding domain significantly reduced autophagic activity, indicating that Beclin 1-mediated autophagy required an interaction with Bcl-2. Overexpression of Bcl-2 had no effect on the autophagic response to nutrient deprivation; however, targeting Bcl-2 to the sarco/endoplasmic reticulum (S/ER) significantly suppressed autophagy. The suppressive effect of S/ER-targeted Bcl-2 was in part due to the depletion of S/ER calcium stores. Intracellular scavenging of calcium by BAPTA-AM significantly blocked autophagy, and thapsigargin, an inhibitor of sarco/endoplasmic reticulum calcium ATPase, reduced autophagic activity by $\sim 50\%$. In cells expressing Bcl-2–ER, thapsigargin maximally reduced autophagic flux. Thus, our results demonstrate that Bcl-2 negatively regulated the autophagic response at the level of S/ER calcium content rather than via direct interaction with Beclin 1. Moreover, we identify calcium homeostasis as an essential component of the autophagic response to nutrient deprivation.

Macroautophagy (hereafter referred to as autophagy) is a highly regulated process by which the cell degrades portions of its cytoplasm and is distinct from chaperone-mediated autophagy and microautophagy [1]. The autophagic process consists of three phases: formation and engulfment, in which portions of the cytoplasm, such as mitochondria and protein aggregates, are surrounded by double-membrane vesicles called autophagosomes; delivery of autophagosomes and their contents to lysosomes; and

Abbreviations
Baf, bafilomycin A_1; E64d, (2*S*,3*S*)-*trans*-epoxysuccinyl-L-leucylamido-3-methylbutane ethyl ester; FM, full medium; GFP, green fluorescent protein; LC3, microtubule-associated protein light chain 3; MKH, modified Krebs–Henseleit buffer; PepA, pepstatin A methyl ester; Rm, rapamycin; S/ER, sarco/endoplasmic reticulum; SERCA, sarco/endoplasmic reticulum calcium ATPase; TG, thapsigargin.

degradation of the autophagosomes and cargo by lysosomal proteases [2,3].

The autophagic pathway is crucial for maintaining cell homeostasis and disruption to the pathway can be a contributing factor to many diseases. Decreased autophagy may promote the development of cancer [4] and neurodegenerative conditions including Alzheimer's [5] and Parkinson's diseases [6]. In the heart, autophagy may protect against apoptosis activated by ischemic injury [7], and its chronic perturbation is causative in a genetic form of heart disease [8]. Conversely, autophagy can also act as a form of programmed cell death linked to, but distinct from, apoptosis [9,10].

Beclin 1, a class III phosphatidylinositol 3-kinase-interacting protein [11], plays a role in promoting autophagy [12]. Beclin 1 contains a Bcl-2-binding domain which may serve as a point of cross-talk between the autophagic and apoptotic pathways. Recently, a BH3 domain in the Bcl-2-binding domain of Beclin 1 was shown to bind to Bcl-X_L [13]. Anti-apoptotic Bcl-2 and Bcl-X_L have been shown to activate the autophagic response during programmed cell death in mouse embryonic fibroblasts [10]. Conversely, Bcl-2 has been shown to suppress starvation-induced autophagy in MCF7 cancer cells [14].

Autophagy begins with formation of the autophagosome. The machinery controlling formation of the autophagosome involves two ubiquitin-like conjugation systems. The first is the conjugation of Atg12 to Atg5 [15]. The other is the processing of the microtubule-associated protein light chain 3 (LC3). Upon activation of autophagy, cytosolic LC3-I undergoes covalent conjugation to phosphatidylethanolamine [16] to form LC-II, which is then recruited into the autophagosome-forming membrane, with Atg12 conjugation to Atg5 as a necessary prerequisite [17]. The recent characterization of green fluorescent protein (GFP)–LC3 is a driving force in the autophagy field as it functions as a unique and specific indicator for autophagosomes in live cells [18]. Currently, demonstration of GFP–LC3 punctae visualized by fluorescence imaging, or LC3-I processing detected by western blotting [18] are widely used methods for detecting changes in autophagic activity and autophagosome formation. However, it is important to note that lysosomal degradation of LC3-II varies according to cell type [19,20]. Moreover, increased numbers of autophagosomes can reflect impaired fusion with lysosomes rather than an upregulation of autophagic activity [21]. Lysosomal degradation of LC3-II is regarded as a more accurate reflection of autophagic activity, and therefore the accumulation of LC3-II in the presence of lysosomal inhibitors is a more accurate indicator of autophagy [20]. For these reasons, studies which rely on steady-state LC3-II concentrations or the steady-state abundance of autophagosomes may reach incorrect conclusions, as increased numbers of autophagosomes do not always correlate with increased autophagic activity.

The goal of this study was to determine the roles of Beclin 1 and Bcl-2 in controlling autophagy. We employed a highly sensitive systematic approach for evaluating autophagy under high-nutrient conditions and in response to nutrient deprivation in the HL-1 cardiac cell line. Active autophagic flux in a cell was determined based upon the increase in GFP–LC3-II accumulation in the presence of lysosomal inhibitors. We found that Bcl-2 has both an activating and suppressive effect on autophagy. Although the Bcl-2-binding domain of Beclin 1 is required for autophagy, Bcl-2 destabilization of sarco/endoplasmic reticulum (S/ER) calcium stores can override Beclin 1 induction of autophagy. These findings reveal additional levels of complexity in the control of autophagy. Physiologic and pathophysiologic implications of this relationship to cardiomyocyte function are discussed.

Results

Inhibiting lysosomal activity to quantify autophagic flux

During the initiation of autophagy, cytosolic LC3 (LC3-I) is cleaved and lipidated to form LC3-II [16,20]. LC3-II is then recruited to the autophagosomal membrane [17]. Transient transfection of the fusion protein, GFP–LC3, allows detection of autophagosomes which appear as punctae by fluorescence microscopy of live or fixed cells.

In this study, we utilized the extent of GFP–LC3-labeled autophagosome formation during a set amount of time as a specific index of macroautophagic activity. To determine the autophagic flux, a lysosomal inhibitor cocktail consisting of the cell-permeable pepstatin A methyl ester (PepA; 5 $\mu g \cdot \mu L^{-1}$, inhibitor of cathepsin D), (2S,3S)-*trans*-epoxysuccinyl-L-leucylamido-3-methylbutane ethyl ester (E64d; 5 $\mu g \cdot \mu L^{-1}$, inhibitor of cathepsin B) and bafilomycin A_1 (Baf; 50 μM; inhibitor of the vacuolar proton ATPase) was used to block lysosomal degradation of autophagosomes [20]. Inhibition of cathepsin activity was verified utilizing the fluorescent MagicRed cathepsin B substrate [22]. Under normal conditions processing of the MagicRed substrate to its fluorescent form by the lysosomal protease cathepsin B allows detection of individual organelles representing the lysosomes. In cells treated with

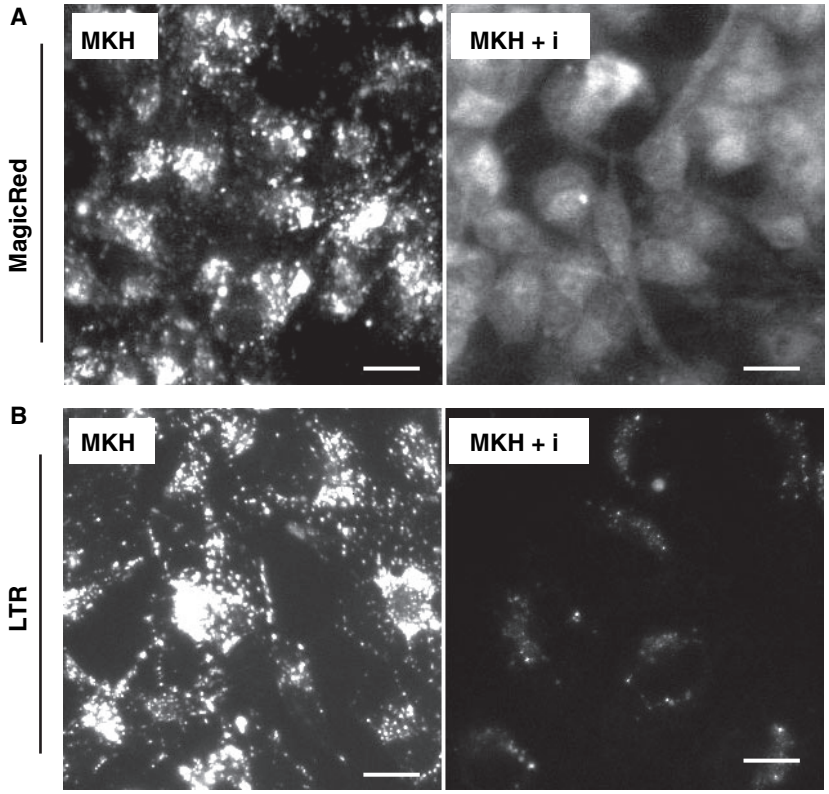

Fig. 1. Inhibition of lysosomal activity with the inhibitor cocktail. (A) Inhibition of cathepsin B activity by lysosomal inhibitors. Activity and intracellular distribution of cathepsin B, a predominant lysosomal protease, was assessed using $(z\text{-}RR)_2$-MagicRed-Cathepsin B substrate (MagicRed). HL-1 cells were treated with lysosomal inhibitors (PepA, E64d and Baf) in MKH buffer for 2 h with MagicRed present during the last 30 min of the experiment, and then imaged. (B) Inhibition of vacuolar proton ATPase activity by lysosomal inhibitors. Following 2 h incubation in MKH + lysosomal inhibitors (MKH + i), cells were loaded with 50 nM LysoTracker Red for 5 min. The buffer was then replaced with dye-free MKH and cells were analyzed by fluorescence microscopy. Scale bar, 20 μm.

the inhibitor cocktail, fluorescence intensity was lower due to decreased MagicRed processing by cathepsin B (Fig. 1A). Similarly, LysoTracker Red, which accumulates in acidic organelles, serves to reveal lysosomal acidification, which is required for protease activity [23] and autophagosome–lysosome fusion [24]. Baf effectively blocked lysosomal acidification (Fig. 1B).

Quantifying autophagy and autophagic flux in HL-1 cardiac myocytes

We first characterized the basal level of autophagy in fully supplemented medium [25]. GFP–LC3-expressing HL-1 cells were incubated without or with lysosomal inhibitor cocktail for 3.5 h. Autophagosomes were visualized by fluorescence microscopy, revealing two distinct populations: cells containing few or no GFP–LC3 punctae ('low'), and a small population of cells exhibiting numerous GFP–LC3 punctae ('high'). To evaluate the effect of rapamycin (Rm), which is known to stimulate autophagy even under high nutrient conditions [26–28], GFP–LC3-expressing HL-1 cells were treated with or without 1 μM Rm in the presence or absence of the lysosomal inhibitors. After 30 min incubation with Rm, cells showed a robust increase in the numbers of GFP–LC3 dots per cell (Fig. 2A, right). Next, we quantified the percentage of cells showing numerous GFP–LC3 dots/cell by fluorescence microscopy. The results, shown in the bar graph (Fig. 2B), indicate the percentage of cells showing numerous GFP–LC3 dots/cell at steady-state. Similar scoring in the presence of the lysosomal inhibitors, allows determination of cumulative autophagosome formation over a defined time interval. The difference in the number of cells with high autophagosome content in the presence or absence of inhibitors (numbers inserted in graphs) represents the percentage of cells with high autophagic flux. Under full medium (FM) conditions, in the presence of lysosomal inhibitors, only a small, statistically insignificant increase in the percentage of cells exhibiting high autophagosome content was observed, indicating low autophagic flux under high nutrient conditions. In contrast, Rm stimulated a significant increase in autophagic flux. Furthermore, our results demonstrate that Rm-stimulated autophagy in FM exceeds the capacity for autophagosome degradation, as steady-state levels of autophagy increased even though flux was greatly enhanced.

In order to further characterize autophagic flux in cell populations, GFP–LC3-expressing cells in FM were treated with or without Rm in the absence of lysosomal inhibitors, and the number of GFP–LC3

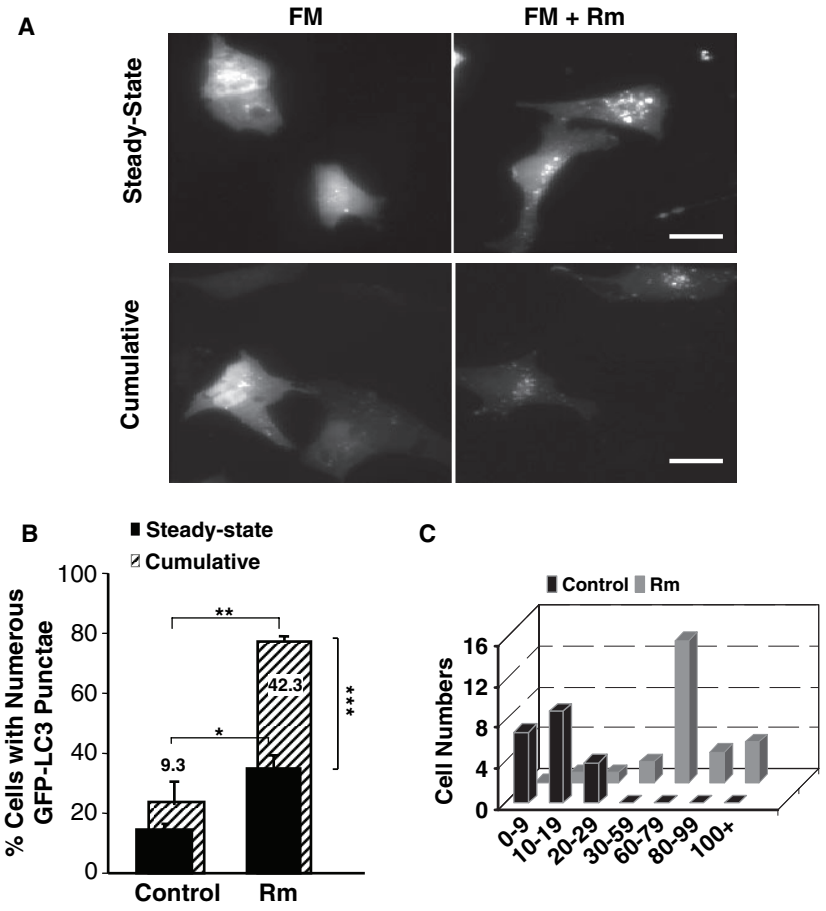

Fig. 2. Basal and Rm-activated autophagic activity in FM. (A) GFP–LC3 transfected HL-1 cells were treated with 1 μM Rm for 30 min in FM, followed by an additional 3.5 h incubation with or without the lysosomal inhibitor cocktail, and fixed with paraformaldehyde. Z-stacks of representative cells were acquired and subsequently processed by 3D blind deconvolution (AutoQuant). Images represent the maximum projections of total cellular GFP–LC3 fluorescence. Scale bar, 15 μm. (B) The percentages of cells with numerous GFP–LC3 punctae at steady state (without lysosomal inhibitor cocktail, solid bars) and cumulative (after incubation with lysosomal inhibitor cocktail, hatched bars) were quantified and compared between FM and Rm-treated. $*P < 0.05$ for Rm versus FM (steady-state); $**P < 0.01$ for Rm versus FM (cumulative); $***P < 0.001$ for Rm versus FM (flux). (C) Population distribution of cells containing various numbers of autophagosomes (X axis, number of autophagosomes per cell) in FM or FM + Rm (without lysosomal inhibitors).

punctae in individual cells was quantified. As shown in Fig. 2C, histogram analysis revealed a bimodal distribution between 'low' and 'high' numbers of GFP–LC3 dots/cell. In the absence of lysosomal inhibitors, the majority of cells had < 20 GFP–LC3 dots/cell and none had > 30 GFP–LC3 dots/cell. In contrast, the majority of cells treated with Rm exhibited > 60 GFP–LC3 dots/cell. Cells with intermediate numbers of autophagosomes were very infrequent. Thus, this distinctive bimodal distribution allows straightforward evaluation of autophagy in a population of cells.

Autophagic response to nutrient deprivation

Autophagy is strongly upregulated in response to nutrient deprivation [19,29]. To examine the autophagic response to starvation in HL-1 cells, GFP–LC3-expressing cells were subjected to nutrient deprivation by incubation in modified Krebs-Henseleit buffer (MKH), which lacks amino acids and serum. Interestingly, after incubation in MKH in the absence of lysosomal inhibitors, most cells exhibited few autophagosomes (Fig. 3), resembling cells incubated in FM (Fig. 2B). This observation in HL-1 cells differs from results in other cell lines [14,20]. However, the addition of lysosomal inhibitors for 3.5 h revealed robust autophagic activity, with $\sim 90\%$ of cells displaying high numbers of GFP–LC3 dots/cell (Fig. 3). The remaining $\sim 10\%$ of cells showed low numbers of GFP–LC3 punctae, possibly because they were in a phase of the cell cycle in which autophagy is suppressed [30,31]. These results demonstrate that autophagic flux was substantially upregulated in HL-1 cells in response to nutrient deprivation, consistent with previous reports [32,33].

Beclin 1 control of the autophagic response to nutrient deprivation requires a functional Bcl-2/-X_L-binding domain

We next investigated the control of Beclin 1 and its binding partner, Bcl-2, on autophagic activity. Beclin 1 was the first mammalian protein described to mediate autophagy [12]. Beclin 1 interaction with the class III

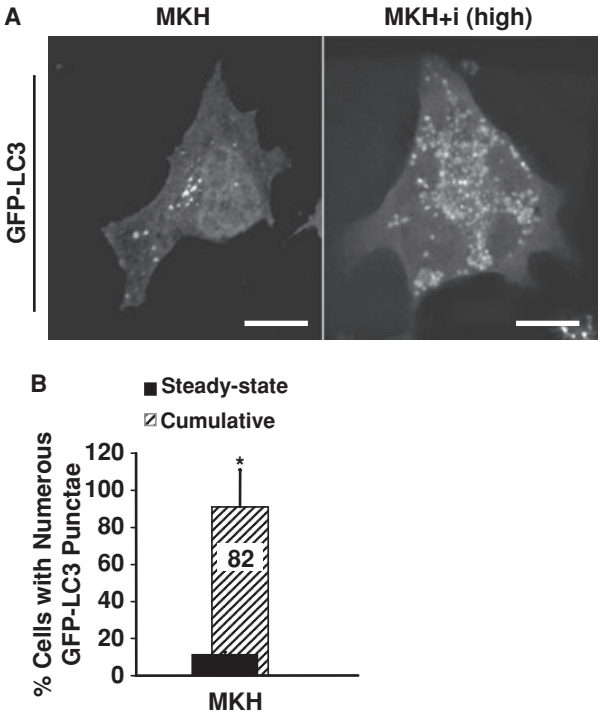

Fig. 3. Autophagic flux under nutrient deprivation. (A) GFP–LC3 transfected HL-1 cells were incubated in low nutrient modified MKH with or without the lysosomal inhibitor cocktail for 3.5 h and fixed with paraformaldehyde. Z-stacks of representative cells were acquired and subsequently processed by 3D blind deconvolution (AutoQuant). Scale bar, 10 μm. (B) The percentages of cells with numerous GFP–LC3 punctae without (steady-state, solid bar) and with lysosomal inhibitors (cumulative, hatched bar) were quantified under conditions of nutrient deprivation (MKH). $*P < 0.001$.

phosphatidylinositol 3-kinase hVps34 is required for activation of the autophagic pathway [34]. Beclin 1 contains a Bcl-2-binding domain which has been shown to interact with antiapoptotic Bcl-2 and Bcl-X_L, but not proapoptotic Bcl-2 family members [35]. However, the nature of the relationship between Beclin 1 and Bcl-2 remains unclear. Recent studies have suggested that Bcl-2 plays a role in the suppression of starvation-induced autophagy [14,36]; others have shown that Bcl-2 positively regulates autophagic cell death activated by etoposide [10].

Here we sought to determine the effect of Beclin 1 and its mutant lacking the Bcl-2-binding domain (Beclin 1ΔBcl2BD) [14] on autophagic activity under high- and low-nutrient conditions. Both Flag–Beclin 1 and its mutant constructs express at comparable levels in HL-1 cells [32]. Under high-nutrient conditions, steady-state and cumulative autophagy were similar between control and Beclin 1-transfected cells (Fig. 4). In MKH buffer, both control and Beclin 1-overexpressing cell populations responded to nutrient deprivation with generalized upregulation of autophagy (Fig. 4). In contrast, Beclin 1ΔBcl2BD expression significantly reduced autophagic flux in both high- and low-nutrient conditions (Fig. 4), indicating that Beclin 1-mediated autophagy required the Bcl-2-binding domain for maximal autophagic response.

Bcl-2 suppression of the autophagic response to nutrient deprivation is dependent on its subcellular localization

Our ability to quantify autophagic flux (versus the commonly reported autophagosome content) revealed the surprising finding that Beclin 1ΔBcl2BD suppressed autophagy. This was in contrast to the studies of Pattingre *et al.* [14], who showed that in cancer cells, Beclin 1ΔBcl2BD, as well as other Beclin 1 mutants lacking the ability to interact with Bcl-2, increased the percentage of cells containing numerous autophagosomes; these mutants have been shown to activate cell death during nutrient deprivation, attributed to excessive autophagy. In addition, they showed that Bcl-2 decreased steady-state autophagy through its interaction with the Beclin 1 Bcl-2-binding domain.

To explore potential reasons for this discrepancy, we quantified autophagic flux in order to evaluate the effect of Bcl-2 overexpression on the response to nutrient deprivation. HL-1 cells were cotransfected with mCherry–LC3 and GFP–Bcl-2-wt (wild-type) or GFP–Bcl-2-ER (S/ER-targeted) (Fig. 5A). Although we found that Beclin 1ΔBcl2BD expression greatly reduced autophagic flux, expression of wild-type Bcl-2 did not alter flux (Fig. 5B). Endogenous Bcl-2 is found in the cytosol, at the mitochondria, and at the S/ER [37]. Forced localization of Bcl-2 to the S/ER has previously been reported to suppress autophagy in response to nutrient deprivation, as indicated by the decrease in the percentage of cells displaying numerous autophagosomes [14]. Our measurement of autophagic activity in the presence and absence of lysosomal inhibitors revealed that Bcl-2-ER, unlike Bcl-2-wt, potently suppressed autophagic flux in response to nutrient deprivation (Fig. 5B).

Bcl-2 overexpression inhibits autophagy due to depletion of sequestered S/ER Ca^{2+} stores

The strong suppressive effect on autophagy exerted by Beclin 1ΔBcl2BD, the profound suppressive effect of Bcl-2-ER, and the minimal suppressive effect of Bcl-2-wt were inconsistent with the notion that Bcl-2 functions as a direct suppressor of Beclin 1 activity. These results suggested the existence of another mechanism

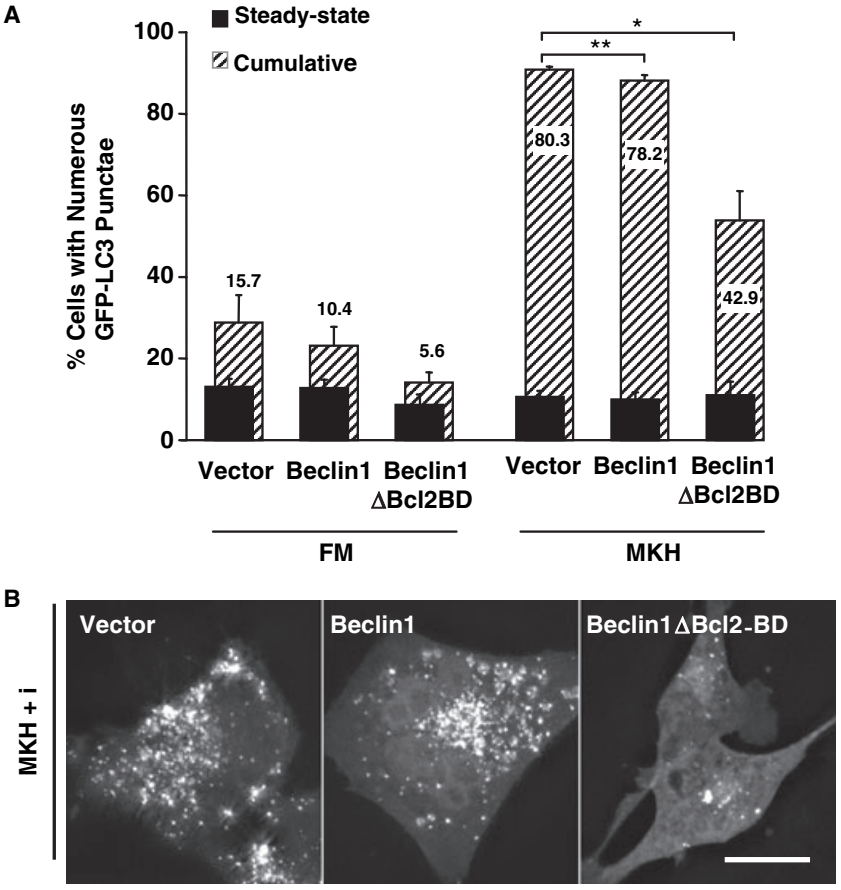

Fig. 4. Beclin 1 regulation of autophagic response. HL-1 cells were cotransfected with GFP–LC3 and a plasmid encoding FLAG–Beclin 1, FLAG–Beclin 1ΔBcl2BD or empty vector, then incubated in either high-nutrient FM or low-nutrient MKH. Parallel wells of cells were incubated without or with the lysosomal inhibitor cocktail, fixed with paraformaldehyde, and imaged. (A) Autophagic flux, quantified by comparison of the percentages of cells with numerous GFP–LC3 dots/cell without (steady-state, black bars) and with lysosomal inhibitors (cumulative, hatched bars), was determined in cells expressing GFP–LC3 and the indicated constructs. $*P < 0.01$ Vector versus Beclin 1ΔBcl2BD (MKH, cumulative); $**P =$ NS vector versus Beclin 1 (MKH, cumulative). (B) Representative images of HL-1 cells incubated in MKH with lysosomal inhibitors (MKH + i) and expressing the indicated constructs. Scale bar, 10 μm.

controlling autophagic activity. Bcl-2 increases the permeability of the S/ER to Ca^{2+} [38] through its interaction with sarco/endoplasmic reticulum calcium ATPase (SERCA), which is responsible for pumping Ca^{2+} from the cytosol back into the S/ER [39]. Intriguingly, S/ER Ca^{2+} stores are required for the activation of autophagy [40] as well as downstream lysosomal function [41]. We hypothesized that Bcl-2 targeted to the S/ER inhibits autophagy in part due to modulation of the S/ER Ca^{2+} content.

We first sought to determine whether overexpression of Bcl-2 significantly reduced Ca^{2+} content in HL-1 cardiac cells. S/ER Ca^{2+} homeostasis is maintained by the opposing processes of release by the ryanodine receptor and re-uptake by SERCA. Thapsigargin (TG), a selective SERCA inhibitor, can be used to deplete S/ER calcium stores by blocking reuptake [42]. Experiments were performed in the presence of norepinephrine (0.1 mM) to stimulate S/ER Ca^{2+} release, and S/ER Ca^{2+} content was inferred by measuring the increase in cytosolic Ca^{2+} 1 min after TG treatment, using the fluorescent Ca^{2+} indicator Fluo-4 (2 μM). TG-mediated depletion of S/ER Ca^{2+} was similar in control and Bcl-2-wt transfected cells, but was significantly reduced in cells transfected with Bcl-2-ER (Fig. 6). These results demonstrate that the capacity for S/ER Ca^{2+} release, an index of S/ER Ca^{2+} content, is reduced by Bcl-2-ER in the HL-1 cardiac myocyte, in agreement with studies performed in other cell lines [39,43].

Positive regulation of autophagy by S/ER Ca^{2+}

We then sought to determine whether low levels of cytosolic Ca^{2+} might influence the activation of autophagy by nutrient deprivation. BAPTA-AM (25 μM), a membrane-permeable Ca^{2+} chelator [44,45], was added to HL-1 cells, and autophagic flux was quantified. BAPTA-AM treatment resulted in nearly complete inhibition of autophagic activity (Fig. 7A). Moreover, BAPTA-AM decreased autophagy even in the presence of Rm (1 μM; results not shown).

To determine whether S/ER Ca^{2+} content affected autophagic activity, we depleted S/ER Ca^{2+} with TG. In control, Bcl-2-wt, and Bcl-2-ER-transfected cells, TG (1 μM) significantly suppressed nutrient deprivation-induced autophagic activity (Fig. 7B).

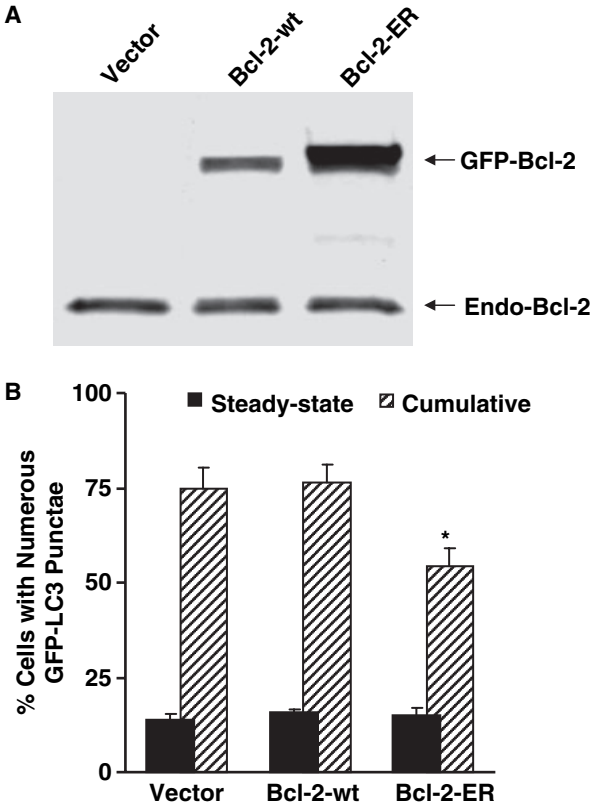

Fig. 5. Bcl-2 control of autophagic activity. HL-1 cells were transfected with mCherry-LC3 and empty vector, GFP–Bcl-2-wt, or GFP–Bcl-2-ER. Experiments were carried out 24 h after transfection. (A) Western blots of cell lysates from transfected cells shows the expression of GFP–Bcl-2 constructs and endogenous Bcl-2 (endo). The whole population of cells from each condition was collected for western blot and therefore includes untransfected cells. Transfection efficiency was noticeably higher with GFP–Bcl-2-ER, accounting for the difference seen on western blot. However, the apparent intensity of fluorescence in cells expressing GFP–Bcl-2-ER was similar to that of GFP–Bcl-2-wt (results not shown), thus allowing us to conclude that differential effects of Bcl-2-ER were due to its localization rather than a difference in expression levels. (B) Cells were incubated in MKH buffer in the absence (steady-state, solid bars) or presence of lysosomal inhibitor cocktail (cumulative, hatched bars) for 3.5 h, then fixed. The accumulation of autophagosomes was quantified only in doubly transfected cells. Flux values are shown in inset boxes. $*P < 0.008$ for Bcl-2-ER versus vector (cumulative).

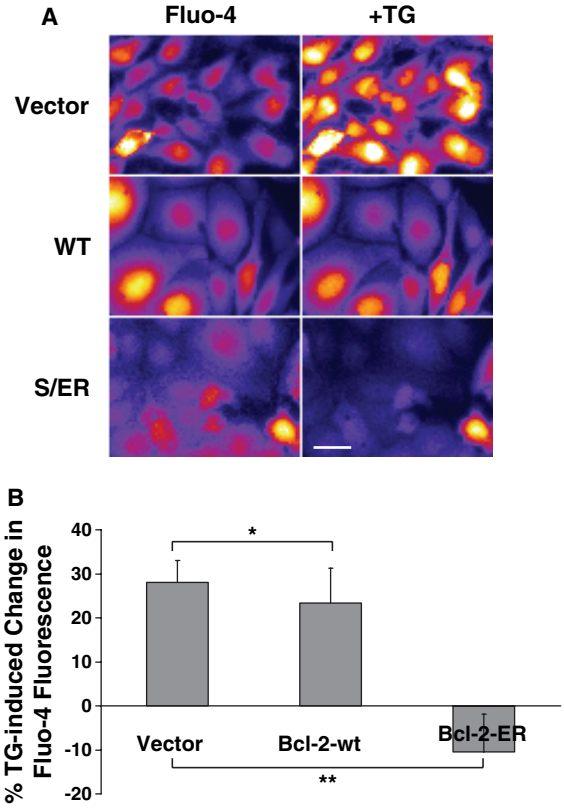

Fig. 6. Bcl-2 localized to the S/ER reduces S/ER calcium content. HL-1 cells were cotransfected with mito-CFP and either Bcl-2-wt or Bcl-2-ER at a ratio of 1 : 3. Cells were incubated with 2 μM Fluo-4 for 20 min followed by washout in dye-free MKH buffer containing norepinephrine (0.1 mM) to facilitate Ca^{2+} cycling. (A) Images were collected before and 1 min after the addition of 1 μM TG (+ TG). Scale bar, 20 μm. (B) The average percent change in Fluo-4 fluorescence after addition of TG was determined. $*P < 0.01$ for vector versus Bcl-2-wt; $**P < 0.001$ for vector versus Bcl-2-ER. The small negative percent change seen with Bcl-2-ER may be due to photobleaching.

Furthermore, in cells expressing Bcl-2-ER, TG reduced autophagic activity to an even greater extent.

Discussion

In this study, we established a method for the quantitative assessment of autophagic activity among a population of cells in order to investigate the control over autophagy exerted by Beclin 1 and its putative interacting partner Bcl-2. By making a distinction between steady-state autophagosome accumulation and autophagic flux, we revealed a complex role for Bcl-2 in the regulation of autophagy: under normal conditions Bcl-2 positively regulates autophagy via its interaction with Beclin 1, yet under conditions in which Bcl-2 is concentrated at the S/ER, the consequent depletion of S/ER lumenal Ca^{2+} results in an overriding inhibition of autophagy.

Determination of autophagic flux

To quantify autophagy in our experimental system, we inhibited lysosomal degradation and analyzed the accumulation of GFP–LC3-positive punctae by fluorescence microscopy. Although stable transfection of GFP–LC3 was reported to increase monodansylcadaverine labeling [46], a fluorescent dye that labels endolyso-

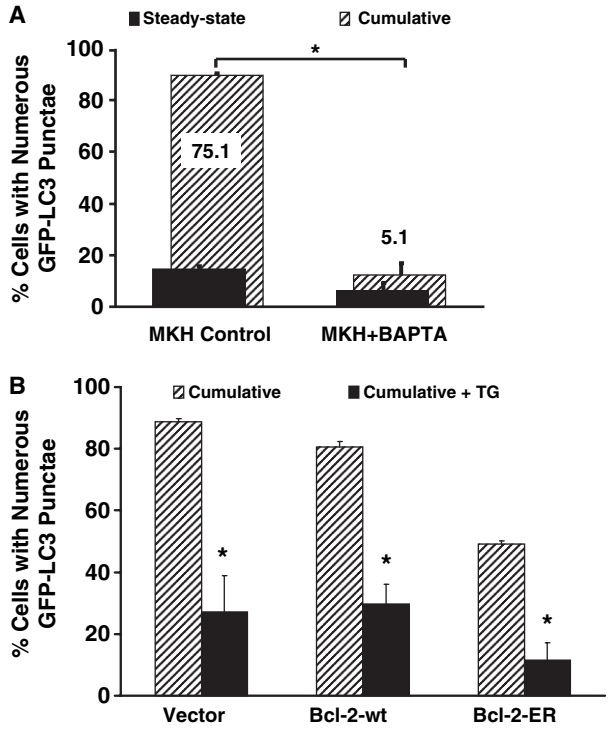

Fig. 7. Role of S/ER Ca^{2+} stores on nutrient deprivation-induced autophagy. HL-1 cells were transfected with GFP–LC3 and incubated in low-nutrient MKH buffer. (A) Cells were incubated without (MKH Control) or with BAPTA-AM (MKH + BAPTA) for 3.5 h; parallel wells were incubated without (steady-state, solid bars) or with (cumulative, hatched bars) lysosomal inhibitors, then fixed and the percentages of cells with numerous GFP–LC3 dots/cell were quantified. $*P < 0.01$, control versus BAPTA (cumulative). Flux values are indicated as inset numbers. (B) Cells were transfected with mito-CFP and either Bcl-2-wt or Bcl-2-ER at a ratio of 1 : 3, then incubated for 3.5 h in low-nutrient MKH buffer, *all* in the presence of lysosomal inhibitors, without (cumulative, open bars) or with 1 μM thapsigargin (cumulative + TG, light gray bars) ($*P < 0.001$, cumulative versus cumulative + TG).

somes [47], it is not known whether GFP–LC3 overexpression truly upregulates autophagy. Importantly, however, transgenic mice expressing GFP–LC3 can develop normally without detectable abnormalities [19]. The application of maximal projections of Z-stacks provides a more complete assessment to detect the number of GFP–LC3-positive dots than that obtained by 2D imaging or electron microscopy, which is limited to the plane of focus or selected intracellular regions. Moreover, unlike commonly used assays measuring degradation of long-lived proteins, the technique we employed is specific to quantify macroautophagy. Such a distinction is relevant, as chaperone-mediated autophagy, which targets cytosolic proteins, is strongly stimulated by ketone bodies, which build up during starvation [48], and by oxidative stress [49]. In fact, recent findings indicate that chaperone-mediated autophagy and macroautophagy may have compensatory functions [50]. In agreement with previous reports [20,51], our results further dispute the widely held assumption that cellular autophagosome numbers correlate with autophagic activity: we show that in response to nutrient deprivation low autophagosome numbers can reflect either high lysosomal turnover of autophagosomes or low autophagic flux. Notably, HL-1 cells in FM (low autophagic activity) or undergoing nutrient deprivation (high autophagic activity) exhibit low steady-state levels of GFP–LC3-positive punctae. This result was surprising, as the upregulation of autophagy by starvation has been reported *in vivo* [19], in isolated primary cells [33], and in other cell lines [52] [14,20]. This discrepancy may be a characteristic of HL-1 cells. The turnover rate of lysosomal degradation may be faster than in other cell types. In addition, the presence of glucose in MKH buffer might have permitted efficient clearance of autophagosomes, in contrast to studies in which glucose, as well as serum and amino acids, was eliminated. We suggest that the best indicator of autophagic activity is flux, which we define as the percentage of cells with numerous autophagosomes after lysosomal inhibition (cumulative), minus the percentage of cells with numerous autophagosomes in the absence of lysosomal inhibitors (steady-state). An increase in steady-state autophagy without a corresponding increase in cumulative autophagy would indicate a defect in autophagosome clearance (a failure to route autophagosome to lysosomes or to degrade them once fused with lysosomes). Conversely, decreased steady-state autophagy in conjunction with decreased cumulative autophagy would indicate impaired formation of autophagosomes. This approach therefore provides additional information about the process of autophagy, revealing points of impairment, and reduces the potential for misinterpretation of results obtained by monitoring LC3–GFP punctae.

Endogenous Bcl-2 enables maximum Beclin 1-mediated autophagic activity during nutrient deprivation

The effect of the interaction between Beclin 1 and Bcl-2/-X_L on autophagic activity is unclear. Control cells exhibited robust autophagic activity in response to nutrient deprivation and Rm, indicating that endogenous levels of Beclin 1 were sufficient to drive maximal autophagic activity. In contrast, the Beclin 1 mutant (Beclin 1ΔBcl2BD) suppressed autophagy, indicating that Beclin 1ΔBcl2BD functioned as a dominant-negative protein during nutrient deprivation. By contrast,

Beclin 1ΔBcl2BD functioned similar to wild-type Beclin 1 to promote clearance of toxic huntingtin aggregates in neurons [53]. Mouse embryonic fibroblasts overexpressing Bcl-2 and Bcl-X_L exhibited increased levels of Atg5–Atg12 conjugates and more GFP–LC3 punctae in response to etoposide [10], and Beclin 1 lacking or mutated in the Bcl-2-binding domain caused a massive accumulation of autophagosomes and induced cell death in both FM and under starvation conditions [14]. In light of our findings that autophagic flux is impaired in cells overexpressing Beclin 1ΔBcl2BD, it is possible to reinterpret the observation of increased numbers of autophagosomes as an indication of impaired autophagolysosomal clearance rather than increased autophagy. Although it is possible that deletion of the Bcl-2-binding domain has a nonspecific effect on Beclin 1 function, we think that our results indicate a requirement for Bcl-2 interaction to promote autophagy. One possible interpretation is that a trimolecular complex, comprising Beclin 1, Bcl-X_L (or Bcl-2), and the class III phosphatidylinositol 3-kinase Vps34, is required for autophagosome formation. In the case of Beclin 1ΔBcl2BD, a nonproductive bimolecular complex (lacking Bcl-2) would form. Beclin 1ΔBcl2BD would compete with Beclin 1 for interaction with Vps34, and in the case of overexpression, would act as a competitive inhibitor.

Pattingre *et al*. [14] showed that autophagosome content was negatively correlated with the amount of Bcl-2 that interacted with Beclin 1, and that Bcl-2 binding of Beclin 1 interfered with the Beclin 1–Vps34 interaction, which signals autophagy. In support of this model, the authors showed that high levels of Bcl-2 and Beclin 1 coimmunoprecipitated under high-nutrient conditions, and conversely, Bcl-2 did not coimmunoprecipitate with Beclin 1 under low-nutrient conditions. However, Zeng *et al*. [54] showed that endogenous Bcl-2 did not interact with Beclin 1 in U-251 cells under FM conditions; only through overexpression of Bcl-2 was such an interaction detected. Moreover, Kihara *et al*. [34] found that under FM conditions all Beclin 1 in HeLa cells is bound to Vps34. These diverging reports raise the possibility that rheostatic control of autophagy by Beclin 1–Bcl−2 interaction is not a universal mechanism. Further experiments are needed to clarify the nature of Bcl-2 control of autophagy at the level of S/ER calcium and Beclin 1 binding.

S/ER-localized Bcl-2 depletes S/ER Ca^{2+}-content, thereby inhibiting autophagy

High S/ER Ca^{2+} stores are required for autophagy [40]. We found that Bcl-2-ER suppressed autophagic activity, similar to the previous report [14] and reduced S/ER Ca^{2+} content, as previously shown [39,43]. Moreover, we directly demonstrated the Ca^{2+} requirement for autophagic activity: intracellular chelation of Ca^{2+} by BAPTA, and depletion of S/ER Ca^{2+} stores by the SERCA inhibitor TG, both profoundly suppressed autophagy. The recent report by Criollo *et al*. [36] found that TG increased the percentage of cells with numerous autophagosomes, which they interpreted as increased autophagic activity. Our studies are consistent with their steady-state observations, but our flux measurements allow us to conclude that TG impairs autophagic flux, and reveal that this effect is in fact related to S/ER Ca^{2+} stores.

Although overexpression of Bcl-2-wt did not suppress autophagy, this may reflect the amount of Bcl-2 localized to the S/ER, which was considerably less than when expressing ER-targeted Bcl-2. We speculate that the specialized S/ER of the HL-1 cardiac myocyte, which contains high SERCA levels, is able to overcome some degree of Bcl-2 leak and maintain S/ER Ca^{2+} content in response to low levels of Bcl-2 [43], yet would be impaired by supra-physiological levels of Bcl-2 at the S/ER [39].

It is interesting to note that the physiological implications of S/ER-targeted Bcl-2 in the cardiac myocyte are unclear. Conditions that trigger preferential recruitment of Bcl-2 to the S/ER have not been shown and it is not known if this might occur under physiologic or pathologic conditions. Although enforced Ca^{2+} release from S/ER stores, by either Bcl-2 or Bcl-X_L, minimizes the Ca^{2+} signaling component of apoptosis [55], it is not known if S/ER targeted-Bcl-2 affects the ability of the cardiac myocyte to contract. While the decrease of S/ER Ca^{2+} stores might be predicted to be harmful to the heart by reducing its capacity to do work, mice overexpressing Bcl-2 in the heart do not exhibit overt cardiac dysfunction [56,57].

The requirement for S/ER Ca^{2+} stores to support autophagy is clear, yet the regulating mechanism remains unknown. Suppression of autophagy by BAPTA buffering of cytosolic Ca^{2+} or by TG-mediated reduction in ER luminal Ca^{2+} suggests that transient S/ER Ca^{2+} release may be a necessary cofactor for activation of autophagy. In this scenario, depending on the nature of amplitude and duration of Ca^{2+} release by TG, its administration could conceivably result in a transient increase in autophagosome formation, followed by a sustained inhibition of autophagic flux. As Vps34 contains a C2 domain, we speculate that transient Ca^{2+} elevations would trigger recruitment of the autophagic machinery to the membrane, in a manner analogous to the recruitment of cytosolic phospholipase A_2 [58]. In addition, it was recently reported that calpain is required for autophagy [59,60],

indirectly implicating calcium necessary to activate calpain. However, this may be a two-edged sword, as it was reported that calpain converts Atg5 to a BH3-only protein capable of triggering apoptosis [61].

Significance in the heart

This study was carried out in the HL-1 cardiac myocyte cell line, which represents a useful model that may extend our understanding of the autophagic processes in the heart. The cardiac myocyte requires an efficient supply and delivery of ATP from the mitochondria to perform work and maintain ion homeostasis. Ca^{2+} couples mitochondrial ATP production to demand: Ca^{2+} release during the action potential stimulates both acto-myosin ATPase activity (contraction) and mitochondrial oxidative phosphorylation [62] through activation of the tricarboxylic acid cycle [63]. Our results reveal that, in addition, Ca^{2+} homeostasis is required for maximal macroautophagic activity in the cardiac myocytes. It is well known that altered Ca^{2+} homeostasis plays a causative role in many forms of cardiovascular disease [64,65]. Our results also suggest that under certain conditions Bcl-2 is required for autophagic activity, supporting previous findings that increased Bcl-2 and autophagic activity correlated with protection in an *in vivo* model of ischemic injury [7,57].

In conclusion, autophagy is emerging as an important process involved in programmed cell death as well as cytoprotection. We suggest that the inability to mount an autophagic response due to depleted S/ER Ca^{2+} is relevant for paradigms of both cellular protection and cell death. The additional insights gained from measurement of autophagic flux may necessarily lead to re-evaluation and reinterpretation of published results. The findings of Levine's [14] and Kroemer's [36] groups in relation to this study clearly illustrate the need to revisit studies in which the steady-state abundance of autophagosomes was used to infer the extent of autophagic activity.

Experimental procedures

Reagents

Rm, BAPTA-AM, PepA, E64d, and Baf were purchased from EMD Biosciences (San Diego, CA); TG was purchased from Sigma (St Louis, MO).

Cell culture and transfections

Cells of the murine atrial-derived cardiac cell line HL-1 [25] were plated in gelatin/fibronectin-coated culture vessels and maintained in Claycomb medium (JRH Biosciences, Lenexa, KS) supplemented with 10% fetal bovine serum, 0.1 mM norepinephrine, 2 mM L-glutamine, 100 $U{\cdot}mL^{-1}$ penicillin, 100 $U{\cdot}mL^{-1}$ streptomycin, and 0.25 $\mu g{\cdot}mL^{-1}$ amphotericin B. Cells were transfected with the indicated vectors using the transfection reagent Effectene (Qiagen, Valencia, CA), according to the manufacturer's instructions, achieving at least 40% transfection efficiency. For experiments aimed at determining autophagic flux, HL-1 cells were transfected with GFP–LC3 and the indicated vector at a ratio of 1 : 3 μg DNA. For calcium imaging experiments, HL-1 cells were transfected with mito-ECFP [66] and the indicated vector at a ratio of 1 : 3 μg DNA.

High- and low-nutrient conditions

Cells were plated in 14-mm-diameter glass bottom microwell dishes (MatTek, Ashland, MA). For high-nutrient conditions, experiments were performed in fully supplemented Claycomb medium. For low-nutrient conditions, experiments were performed in modified MKH (in mM: 110 NaCl, 4.7 KCl, 1.2 KH_2PO_4, 1.25 $MgSO_4$, 1.2 $CaCl_2$, 25 $NaHCO_3$, 15 glucose, 20 Hepes, pH 7.4) and incubation at 95% room air–5% CO_2.

Wide-field fluorescence microscopy

Cells were observed through a Nikon TE300 fluorescence microscope (Nikon, Melville, NY) equipped with a ×10 lens (0.3 NA, Nikon), a ×40 Plan Fluor and a ×60 Plan Apo objective (1.4 NA and 1.3 NA oil immersion lenses; Nikon), a Z-motor (ProScanII, Prior Scientific, Rockland, MA), a cooled CCD camera (Orca-ER, Hamamatsu, Bridgewater, NJ) and automated excitation and emission filter wheels controlled by a LAMBDA 10–2 (Sutter Instrument, Novato, CA) operated by MetaMorph 6.2r4 (Molecular Devices Co., Downington, PA). Fluorescence was excited through an excitation filter for fluorescein isothiocyanate (HQ480/×40), and Texas Red (D560/×40). Fluorescent light was collected via a polychroic beamsplitter (61002 bs) and an emission filter for fluorescein isothiocyanate (HQ535/50 m), and Texas Red (D630/60 m). All filters were from Chroma. Acquired wide-field Z-stacks were routinely deconvolved using 10 iterations of a 3D blind deconvolution algorithm (AutoQuant) to maximize spatial resolution. Unless stated otherwise, representative images shown are maximum projections of Z-stacks taken with 0.3 μm increments capturing total cellular volume.

Determination of autophagic content and flux

To analyze autophagic flux, GFP–LC3-expressing cells were subjected to the indicated experimental conditions with and without a cocktail of the cell-permeable lysosomal inhibitors

Baf (50 nM, vacuolar H^+-ATPase inhibitor) to inhibit autophagosome–lysosome fusion [24], and E64d (5 $\mu g \cdot mL^{-1}$, inhibitor of cysteine proteases, including cathepsin B), and PepA (5 $\mu g \cdot mL^{-1}$, cathepsin D inhibitor) to inhibit lysosomal protease activity, for an interval of 3.5 h. Cells were fixed with 4% formaldehyde in NaCl/P_i (pH 7.4) for 15 min.

To quantify the number of GFP–LC3 punctae in a single cell, Z-stack images of single GFP–LC3-expressing cells were captured using ×60 oil objective and then background fluorescence was removed by applying a mean filter (4-pixel) to each stack image. Maximal projection images were produced, and the number of GFP–LC3 punctae per cell was determined using IMAGEJ software (NIH, Bethesda, MD). For population analysis, cells were inspected at 60× magnification and classified as: (a) cells with predominantly diffuse GFP–LC3 fluorescence; or as (b) cells with numerous GFP–LC3 punctae (> 30 dots/cell), representing autophagosomes. At least 200 cells were scored for each condition in three or more independent experiments.

Determining the activity of the lysosomal compartment

LysoTracker Red is a cell-permeable acidotropic probe that selectively labels vacuoles with low internal pH and thus can be used to label functional lysosomes. Following sI/R and control experiments, cells were loaded with 50 nM LysoTracker Red for 5 min in MKH; the medium was then exchanged with dye-free MKH, and cells were imaged at ×40 magnification by fluorescence microscopy. Activity and intracellular distribution of cathepsin B, a predominant lysosomal protease, was assessed using $(z\text{-}RR)_2$-MagicRed-Cathepsin B substrate (B-Bridge International, Inc., Mountain View, CA). MagicRed-Cathepsin B substrate was added to the cells during the last 30 min of an experiment according to the manufacturer's instructions.

Calcium imaging

For dye loading, Fluo-4 was dissolved in in 20% (w/v) Pluronic F-127 in dimethylsulfoxide (Invitrogen, Carlsbad, CA; #P-300MP) to a 2 mM stock Fluo-4/AM solution. Cells were incubated for 20 min in 2 μM Fluo-2/AM at 37 °C in MKH buffer. Then the dye-containing solution was replaced with dye-free MKH buffer containing 0.1 mM norepinephrine and cells were incubated for a further 30 min at 37 °C prior to imaging. Mito-CFP-transfected cells were selected and 10 consecutive images ($1 \cdot s^{-1}$) of Fluo-4 were acquired. TG (1 μM) was then added, allowed to incubate for 1 min, and subsequently 10 consecutive images ($1 \cdot s^{-1}$) of Fluo-4 fluorescence were acquired. The average change in Fluo-4 fluorescence (F) intensity ($F_{initial}/(F_{final} - F_{initial})$) was determined from cellular image intensities using the IMAGEJ multi-ROI function (rsb.info.nih.gov/ij).

Western blotting

Whole-cell lysates were subjected to 10–20% trisglycine SDS/PAGE and transferred to nitrocellulose membranes. Blots were probed with anti-Bcl-2 serum (C-2, 1 : 200, Santa Cruz Biotechnology, Santa Cruz, CA) or anti-Beclin 1 serum (1 : 200).

Statistics

The probability of statistically significant differences between two experimental groups was determined by Student's t-test. Values are expressed as mean ± SEM of at least three independent experiments unless stated otherwise.

Acknowledgements

HL-1 cells were kindly provided by Dr William Claycomb (LSU Health Sciences Center, Louisiana). We would like to thank Dr Clark Distelhorst (Case Western Reserve University, Cleveland, Ohio) for providing the Bcl-2 constructs, Dr Roger Tsien (University of California, San Diego) for providing pRSET-mCherry, Dr Beth Levine (University of Texas Southwestern, Texas) for providing the Beclin 1 constructs, including Beclin 1ΔBcl2-BD, and Dr Tamotsu Yoshimori (National Institute of Genetics, Japan) for providing GFP–LC3. This study was supported by the NIH grants R01-AG21568 and R01-HL60590 (to RAG) and the Stein endowment fund. This is MS#18259 of The Scripps Research Institute.

References

1 Cuervo AM (2004) Autophagy: many paths to the same end. *Mol Cell Biochem* **263**, 55–72.
2 Stromhaug PE & Klionsky DJ (2001) Approaching the molecular mechanism of autophagy. *Traffic* **2**, 524–531.
3 Mizushima N, Ohsumi Y & Yoshimori T (2002) Autophagosome formation in mammalian cells. *Cell Struct Funct* **27**, 421–429.
4 Yue Z, Jin S, Yang C, Levine AJ & Heintz N (2003) *Beclin 1*, an autophagy gene essential for early embryonic development, is a haploinsufficient tumor suppressor. *Proc Natl Acad Sci USA* **100**, 15077–15082.
5 Nixon RA, Wegiel J & Kumar A, Yu WH, Peterhoff C, Cataldo A & Cuervo AM (2005) Extensive involvement of autophagy in Alzheimer disease: an immuno-electron microscopy study. *J Neuropathol Exp Neurol* **64**, 113–122.
6 Webb JL, Ravikumar B, Atkins J, Skepper JN & Rubinsztein DC (2003) Alpha-synuclein is degraded by both autophagy and the proteasome. *J Biol Chem* **278**, 25009–25013.

7 Yan L, Vatner DE, Kim SJ, Ge H, Masurekar M, Massover WH, Yang G, Matsui Y, Sadoshima J & Vatner SF (2005) Autophagy in chronically ischemic myocardium. *Proc Natl Acad Sci USA* **102**, 13807–13812.

8 Saftig P, Tanaka Y, Lullmann-Rauch R & von Figura K (2001) Disease model: LAMP-2 enlightens Danon disease. *Trends Mol Med* **7**, 37–39.

9 Xue L, Fletcher GC & Tolkovsky AM (2001) Mitochondria are selectively eliminated from eukaryotic cells after blockade of caspases during apoptosis. *Curr Biol* **11**, 361–365.

10 Shimizu S, Kanaseki T, Mizushima N, Mizuta T, Arakawa-Kobayashi S, Thompson CB & Tsujimoto Y (2004) Role of Bcl-2 family proteins in a non-apoptotic programmed cell death dependent on autophagy genes. *Nat Cell Biol* **6**, 1221–1228.

11 Furuya N, Yu J, Byfield M, Pattingre S & Levine B (2005) The evolutionarily conserved domain of Beclin 1 is required for Vps34 binding, autophagy and tumor suppressor function. *Autophagy* **1**, 46–52.

12 Liang XH, Jackson S, Seaman M, Brown K, Kempkes B, Hibshoosh H & Levine B (1999) Induction of autophagy and inhibition of tumorigenesis by beclin 1. *Nature* **402**, 672–676.

13 Oberstein A, Jeffrey P & Shi Y (2007) Crystal structure of the BCL–XL–beclin 1 peptide complex: beclin 1 is a novel BH3-only protein. *J Biol Chem* **282**, 13123–13132.

14 Pattingre S, Tassa A, Qu X, Garuti R, Liang XH, Mizushima N, Packer M, Schneider MD & Levine B (2005) Bcl-2 antiapoptotic proteins inhibit Beclin 1-dependent autophagy. *Cell* **122**, 927–939.

15 Mizushima N, Noda T, Yoshimori T, Tanaka Y, Ishii T, George MD, Klionsky DJ, Ohsumi M & Ohsumi Y (1998) A protein conjugation system essential for autophagy. *Nature* **395**, 395–398.

16 Kabeya Y, Mizushima N, Yamamoto A, Oshitani-Okamoto S, Ohsumi Y & Yoshimori T (2004) LC3, GABARAP and GATE16 localize to autophagosomal membrane depending on form-II formation. *J Cell Sci* **117**, 2805–2812.

17 Mizushima N, Yamamoto A, Hatano M, Kobayashi Y, Kabeya Y, Suzuki K, Tokuhisa T, Ohsumi Y & Yoshimori T (2001) Dissection of autophagosome formation using Apg5-deficient mouse embryonic stem cells. *J Cell Biol* **152**, 657–668.

18 Kabeya Y, Mizushima N, Ueno T, Yamamoto A, Kirisako T, Noda T, Kominami E, Ohsumi Y & Yoshimori T (2000) LC3, a mammalian homologue of yeast Apg8p, is localized in autophagosome membranes after processing. *EMBO J* **19**, 5720–5728.

19 Mizushima N, Yamamoto A, Matsui M, Yoshimori T & Ohsumi Y (2004) *In vivo* analysis of autophagy in response to nutrient starvation using transgenic mice expressing a fluorescent autophagosome marker. *Mol Biol Cell* **15**, 1101–1111.

20 Tanida I, Minematsu-Ikeguchi N, Ueno T & Kominami E (2005) Lysosomal turnover, but not a cellular level, of endogenous LC3 is a marker for autophagy. *Autophagy* **1**, 84–91.

21 Webb JL, Ravikumar B & Rubinsztein DC (2004) Microtubule disruption inhibits autophagosome–lysosome fusion: implications for studying the roles of aggresomes in polyglutamine diseases. *Int J Biochem Cell Biol* **36**, 2541–2550.

22 Lamparska-Przybysz M, Gajkowska B & Motyl T (2005) Cathepsins and BID are involved in the molecular switch between apoptosis and autophagy in breast cancer MCF-7 cells exposed to camptothecin. *J Physiol Pharmacol 56 Suppl 3*, 159–179.

23 Yoshimori T, Yamamoto A, Moriyama Y, Futai M & Tashiro Y (1991) Bafilomycin A1, a specific inhibitor of vacuolar-type H(+)-ATPase, inhibits acidification and protein degradation in lysosomes of cultured cells. *J Biol Chem* **266**, 17707–17712.

24 Yamamoto A, Tagawa Y, Yoshimori T, Moriyama Y, Masaki R & Tashiro Y (1998) Bafilomycin A1 prevents maturation of autophagic vacuoles by inhibiting fusion between autophagosomes and lysosomes in rat hepatoma cell line, H-4-II-E cells. *Cell Struct Funct* **23**, 33–42.

25 Claycomb WC, Lanson NA Jr, Stallworth BS, Egeland DB, Delcarpio JB, Bahinski A & Izzo NJ Jr (1998) HL-1 cells: a cardiac muscle cell line that contracts and retains phenotypic characteristics of the adult cardiomyocyte. *Proc Natl Acad Sci USA* **95**, 2979–2984.

26 Noda T & Ohsumi Y (1998) Tor, a phosphatidylinositol kinase homologue, controls autophagy in yeast. *J Biol Chem* **273**, 3963–3966.

27 Schmelzle T & Hall MN (2000) TOR, a central controller of cell growth. *Cell* **103**, 253–262.

28 Ravikumar B, Vacher C, Berger Z, Davies JE, Luo S, Oroz LG, Scaravilli F, Easton DF, Duden R, O'Kane CJ *et al.* (2004) Inhibition of mTOR induces autophagy and reduces toxicity of polyglutamine expansions in fly and mouse models of Huntington disease. *Nat Genet* **36**, 585–595.

29 Levine B & Yuan J (2005) Autophagy in cell death: an innocent convict? *J Clin Invest* **115**, 2679–2688.

30 Eskelinen EL, Prescott AR, Cooper J, Brachmann SM, Wang L, Tang X, Backer JM & Lucocq JM (2002) Inhibition of autophagy in mitotic animal cells. *Traffic* **3**, 878–893.

31 Arai K, Ohkuma S, Matsukawa T & Kato S (2001) A simple estimation of peroxisomal degradation with green fluorescent protein – an application for cell cycle analysis. *FEBS Lett* **507**, 181–186.

32 Hamacher-Brady A, Brady NR & Gottlieb RA (2006) Enhancing macroautophagy protects against ischemia/reperfusion injury in cardiac myocytes. *J Biol Chem* **281**, 29776–29787.

33 Kochl R, Hu XW, Chan EY & Tooze SA (2006) Microtubules facilitate autophagosome formation and fusion of autophagosomes with endosomes. *Traffic* **7**, 129–145.
34 Kihara A, Kabeya Y, Ohsumi Y & Yoshimori T (2001) Beclin–phosphatidylinositol 3-kinase complex functions at the *trans*-Golgi network. *EMBO Rep* **2**, 330–335.
35 Liang XH, Kleeman LK, Jiang HH, Gordon G, Goldman JE, Berry G, Herman B & Levine B (1998) Protection against fatal Sindbis virus encephalitis by beclin, a novel Bcl-2-interacting protein. *J Virol* **72**, 8586–8596.
36 Criollo A, Maiuri MC, Tasdemir E, Vitale I, Fiebig AA, Andrews D, Molgo J, Diaz J, Lavandero S, Harper F *et al*. (2007) Regulation of autophagy by the inositol trisphosphate receptor. *Cell Death Differ* **14**, 1029–1039.
37 Lithgow T, van Driel R, Bertram JF & Strasser A (1994) The protein product of the oncogene *bcl-2* is a component of the nuclear envelope, the endoplasmic reticulum, and the outer mitochondrial membrane. *Cell Growth Differ* **5**, 411–417.
38 Foyouzi-Youssefi R, Arnaudeau S, Borner C, Kelley WL, Tschopp J, Lew DP, Demaurex N & Krause KH (2000) Bcl-2 decreases the free Ca^{2+} concentration within the endoplasmic reticulum. *Proc Natl Acad Sci USA* **97**, 5723–5728.
39 Dremina ES, Sharov VS, Kumar K, Zaidi A, Michaelis EK & Schoneich C (2004) Anti-apoptotic protein Bcl-2 interacts with and destabilizes the sarcoplasmic/endoplasmic reticulum Ca^{2+}-ATPase (SERCA). *Biochem J* **383**, 361–370.
40 Gordon PB, Holen I, Fosse M, Rotnes JS & Seglen PO (1993) Dependence of hepatocytic autophagy on intracellularly sequestered calcium. *J Biol Chem* **268**, 26107–26112.
41 Hoyer-Hansen M, Bastholm L, Mathiasen IS, Elling F & Jaattela M (2005) Vitamin D analog EB1089 triggers dramatic lysosomal changes and Beclin 1-mediated autophagic cell death. *Cell Death Differ* **12**, 1297–1309.
42 Thastrup O, Cullen PJ, Drobak BK, Hanley MR & Dawson AP (1990) Thapsigargin, a tumor promoter, discharges intracellular Ca^{2+} stores by specific inhibition of the endoplasmic reticulum Ca2(+)-ATPase. *Proc Natl Acad Sci USA* **87**, 2466–2470.
43 Palmer AE, Jin C, Reed JC & Tsien RY (2004) Bcl-2-mediated alterations in endoplasmic reticulum Ca^{2+} analyzed with an improved genetically encoded fluorescent sensor. *Proc Natl Acad Sci USA* **101**, 17404–17409.
44 Savina A, Fader CM, Damiani MT & Colombo MI (2005) Rab11 promotes docking and fusion of multivesicular bodies in a calcium-dependent manner. *Traffic* **6**, 131–143.
45 Nakano T, Inoue H, Fukuyama S, Matsumoto K, Matsumura M, Tsuda M, Matsumoto T, Aizawa H & Nakanishi Y (2006) Niflumic acid suppresses interleukin-13-induced asthma phenotypes. *Am J Respir Crit Care Med* **173**, 1216–1221.
46 Munafo DB & Colombo MI (2002) Induction of autophagy causes dramatic changes in the subcellular distribution of GFP–Rab24. *Traffic* **3**, 472–482.
47 Bampton ET, Goemans CG, Niranjan D, Mizushima N & Tolkovsky AM (2005) The dynamics of autophagy visualized in live cells: from autophagosome formation to fusion with endo/lysosomes. *Autophagy* **1**, 23–36.
48 Finn PF & Dice JF (2005) Ketone bodies stimulate chaperone-mediated autophagy. *J Biol Chem* **280**, 25864–25870.
49 Kiffin R, Christian C, Knecht E & Cuervo AM (2004) Activation of chaperone-mediated autophagy during oxidative stress. *Mol Biol Cell* **15**, 4829–4840.
50 Massey AC, Kaushik S, Sovak G, Kiffin R & Cuervo AM (2006) Consequences of the selective blockage of chaperone-mediated autophagy. *Proc Natl Acad Sci USA* **103**, 5805–5810.
51 Kovacs AL & Seglen PO (1982) Inhibition of hepatocytic protein degradation by inducers of autophagosome accumulation. *Acta Biol Med Ger* **41**, 125–130.
52 Jager S, Bucci C, Tanida I, Ueno T, Kominami E, Saftig P & Eskelinen EL (2004) Role for Rab7 in maturation of late autophagic vacuoles. *J Cell Sci* **117**, 4837–4848.
53 Shibata M, Lu T, Furuya T, Degterev A, Mizushima N, Yoshimori T, Macdonald M, Yankner B & Yuan J (2006) Regulation of intracellular accumulation of mutant Huntingtin by Beclin 1. *J Biol Chem* **281**, 14474–14485.
54 Zeng X, Overmeyer JH & Maltese WA (2006) Functional specificity of the mammalian Beclin–Vps34–PI 3-kinase complex in macroautophagy versus endocytosis and lysosomal enzyme trafficking. *J Cell Sci* **119**, 259–270.
55 Chami M, Prandini A, Campanella M, Pinton P, Szabadkai G, Reed JC & Rizzuto R (2004) Bcl-2 and Bax exert opposing effects on Ca^{2+} signaling, which do not depend on their putative pore-forming region. *J Biol Chem* **279**, 54581–54589.
56 Chen Z, Chua CC, Ho YS, Hamdy RC & Chua BH (2001) Overexpression of Bcl-2 attenuates apoptosis and protects against myocardial I/R injury in transgenic mice. *Am J Physiol Heart Circ Physiol* **280**, H2313–H2320.
57 Brocheriou V, Hagege AA, Oubenaissa A, Lambert M, Mallet VO, Duriez M, Wassef M, Kahn A, Menasche P & Gilgenkrantz H (2000) Cardiac functional improvement by a human Bcl-2 transgene in a mouse model of ischemia/reperfusion injury. *J Gene Med* **2**, 326–333.
58 Rizo J & Sudhof TC (1998) C2-domains, structure and function of a universal Ca^{2+}-binding domain. *J Biol Chem* **273**, 15879–15882.

59 Demarchi F, Bertoli C, Copetti T, Tanida I, Brancolini C, Eskelinen EL & Schneider C (2006) Calpain is required for macroautophagy in mammalian cells. *J Cell Biol* **175**, 595–605.
60 Demarchi F, Bertoli C, Copetti T, Eskelinen EL & Schneider C (2007) Calpain as a novel regulator of autophagosome formation. *Autophagy* **3**, 235–237.
61 Yousefi S, Perozzo R, Schmid I, Ziemiecki A, Schaffner T, Scapozza L, Brunner T & Simon HU (2006) Calpain-mediated cleavage of Atg5 switches autophagy to apoptosis. *Nat Cell Biol* **8**, 1124–1132.
62 Duchen MR (2000) Mitochondria and calcium: from cell signalling to cell death. *J Physiol* **529**, 57–68.
63 Rizzuto R, Bernardi P & Pozzan T (2000) Mitochondria as all-round players of the calcium game. *J Physiol* **529**, 37–47.
64 Birkeland JA, Sejersted OM, Taraldsen T & Sjaastad I (2005) EC-coupling in normal and failing hearts. *Scand Cardiovasc J* **39**, 13–23.
65 Belke DD & Dillmann WH (2004) Altered cardiac calcium handling in diabetes. *Curr Hypertens Rep* **6**, 424–429.
66 Brady NR, Hamacher-Brady A & Gottlieb RA (2006) Proapoptotic BCL-2 family members and mitochondrial dysfunction during ischemia/reperfusion injury, a study employing cardiac HL-1 cells and GFP biosensors. *Biochim Biophys Acta* **1757**, 667–678.